coatings

MDPI

Review

Recent Progress on Boosting the Perovskite Film Quality of All-Inorganic Perovskite Solar Cells

Ying Chen [1,2,*], Fuqiang Li [1,2], Man Zhang [3] and Zhenyuan Yang [1,2]

[1] Hubei Engineering Technology Research Center of Energy Photoelectric Device and System, Hubei University of Technology, Wuhan 430068, China
[2] School of Science, Hubei University of Technology, Wuhan 430068, China
[3] School of Electrical and Electronic Engineering, Hubei University of Technology, Wuhan 430068, China
* Correspondence: chenyddc@163.com

Abstract: All-inorganic $CsPbX_3$ perovskite material not only has the benefits of advanced light absorption coefficient, long carrier lifetime, and simple preparation process of organic–inorganic perovskite materials but it also maintains excellent stability under the erosion of damp heat. Stability is the premise of its industrialization, so all-inorganic perovskite is undoubtedly a very competitive direction for the development of perovskite materials. However, there are still many defects in the all-inorganic perovskite thin films, and it is difficult to obtain high power conversion efficiency (PCE). This review systematically summarizes additive engineering, solvent engineering, and interface engineering methods to promote the thin film property for a high PCE in recent years.

Keywords: perovskite film preparation; all-inorganic; perovskite solar cells; $CsPbX_3$

Citation: Chen, Y.; Li, F.; Zhang, M.; Yang, Z. Recent Progress on Boosting the Perovskite Film Quality of All-Inorganic Perovskite Solar Cells. *Coatings* **2023**, *13*, 281. https://doi.org/10.3390/coatings13020281

Academic Editor: Natalia V. Kamanina

Received: 19 December 2022
Revised: 15 January 2023
Accepted: 24 January 2023
Published: 26 January 2023

1. Introduction

Perovskite materials have attracted widespread attention in recent years due to their high light absorption coefficient, long carrier lifetime, low cost, simple preparation process [1–4], and ability for large-scale preparation [5–8]. The organic–inorganic hybrid perovskite solar cells (PSCs) have rapidly increased their power conversion efficiency (PCE) from 9.7% to over 25.5% [9–12]. However, in organic–inorganic hybrid perovskite devices, their organic parts, such as MA^+ ($CH_3NH_3^+$), FA^+ ($((CH(NH)_2)_2^+$), are easily affected and decomposed by the external temperature, illumination, and humidity [1,13–17], which leads to a serious decline in the PCE and stability [2,18]. For example, Juarez-Perez et al. [19] reported the decomposition temperature of MA^+ was 80 °C, which was in the operating temperature range of PSCs. In 2015, Eperon et al. [20] for the first time prepared the all-inorganic $CsPbI_3$ cell and the PCE was 2.9%. This historic breakthrough provided a new idea to develop the PSCs. Liu et al. [21] revealed the PSCs based on Cs-doped $MAPbI_3$ can work steadily at 85 °C for 1000 h. They have manufactured modules (6.5 cm × 7 cm) with an advanced PCE of 21.08%. Steele et al. [22] found black $CsPbI_3$ was stable even at a high temperature of 330 °C. All-inorganic perovskite also showed smaller exciton binding energy, higher defect tolerance, and better photoelectric property [23–25]. In particular, a $CsPbI_3$ battery with an appropriate forbidden bandwidth of ~1.73 eV for the roof of a battery with silicon or other narrow band gap formation series battery [26,27]. All-inorganic perovskite solar cells have aroused wide public concern, as the PCE went to 21.0% in just a few years [28–33]. Although all-inorganic PSCs exhibited many excellent properties, their long-term development also faces many challenges, such as poor phase stability, high-density defects, and lower PCE. The property of the all-inorganic perovskite film affects the capability of the solar cells directly [34,35]. This review summarizes the main methods to obtain high-property all-inorganic perovskite films, including additive engineering, solvent engineering, and interface engineering. Then, we prospected the research direction and development prospect of all-inorganic PSCs in the future.

2. Film Quality Improvement

2.1. Additive Engineering

ABX_3 (A = Cs^+, B = Pb^{2+}, X = I^-, Br^-, Cl^-) is the general formula crystal structure for all-inorganic perovskite materials [1,14,36–38]. As shown in Figure 1, there are four common crystal structures: the cubic phase (α-, Pm3m), the tetragonal phase (β-, P4/mbm), the orthorhombic phase (γ-, Pbnm), and the non-perovskite phase (δ-, Pnma) [39,40]. α, β, and γ phases are perovskite phases, and have a photovoltaic effect. They are also called black phases. However, they are only stable at high temperatures. At room temperature, these black perovskite phases will naturally transform into the yellow non-perovskite phase, which will seriously affect the performance of the PSCs [5,41]. The perovskite crystal structure stability can be calculated by the tolerance factor t: $t = (R_A + R_B)/\sqrt{2}(R_B + R_X)$, where R_A, R_B, and R_X refer to the ionic radii of A, B, and X site ions, separately. Under normal conditions, if the crystal wants to maintain stability, the tolerance factor t needs to be in the range of 0.9–1. If the t value is less than this range, the crystal symmetry will be reduced and the entire structure stability will be affected. If the t value is more than this range, the system will occur a certain phase transition [38,42–44]. Therefore, in the research of all-inorganic perovskites, there is a certain theoretical basis for the selection of ions.

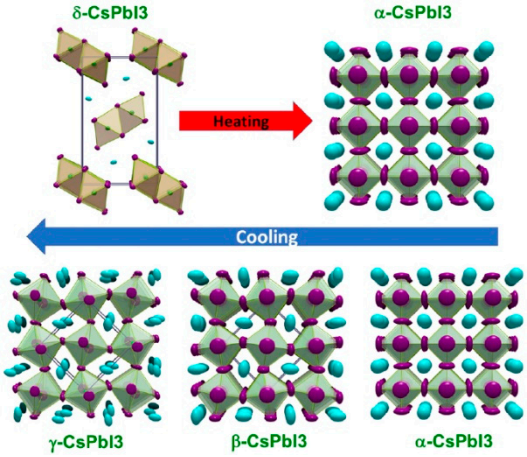

Figure 1. Four different structural phases of $CsPbI_3$ and their phase transitions reprinted with permission from Ref. [39] 2018 American Chemical Society.

The method of additive engineering is an easy way to raise the stability of $CsPbX_3$ perovskite solar cells. Based on the tolerance factor t, lesser X-site anions mean bigger t values. The Br^- (1.96 Å) and Cl^- (1.81 Å) both have a smaller radius than I^- (2.2 Å), so some groups have added them into $CsPbI_3$. The $CsPbI_3$ structural stability increased with the bigger t values [9,25,26,45–51]. The SCN^- ion, a kind of pseudohalide ion, has a smaller radius, which could also strengthen the crystallization behavior of the $CsPbI_3$ film, and promoted the PCE to 17.03% [52]. Wang et al. [53] resoundingly synthesized high-property $CsPbBr_3$ films by adding 1.5% of NH_4SCN into the precursor solution, which contained $NH4^+$ and pseudohalide ion SCN^-.

The lesser B-site cations are also good for phase stability [54]. Sn^{2+} and Pb^{2+} are both from group IVA and have similar physicochemical properties. The smaller Sn^{2+} ionic radius means a bigger t value, giving higher phase stability. Thus, Sn^{2+} is the most hopeful candidate to replace Pb^{2+}. Murugadoss et al. [55] used different concentrations of Sn^{2+} doping to synthesize highly stable black phase $CsPbI_3$ films, improving the PCE to 5.12%. The alkali metal ions from the group IIA, such as Ca^{2+} [56], Sr^{2+} [57], and Ba^{2+} [58,59], have the same valence state as Pb^{2+}, which are also potential competitors. In addition, Mn^{2+} could improve the stability of $CsPbI_3$ perovskite effectively [60–62]. Xu et al. found the appropriate amount of Cd^{2+} (1.0% mol of Pb^{2+}) could improve the crystallinity of $CsPbIBr_2$, reduce its trap density, and suppress its photo-generated carrier

recombination [63]. The trivalent smaller cations could also replace the B-site. Typical trivalent ions are Bi^{3+} [64], Sb^{3+} [65], Yb^{3+} [66], Eu^{3+} [67], In^{3+} [18], Er^{3+} [68], and Gd^{3+} [69]. Faheem et al. [68] deposited a series of different concentrations of trivalent anion Er^{3-} into $CsPbIBr_2$ perovskite. They found $CsI\text{-}(PbBr_2)_{0.97}$ $(ErCl_3)_{0.03}$ was the optimal ratio. The PCE of this solar cell was increased by about 60% (7.28%). Pu et al. [69] used different molar ratios of gadolinium chloride ($GdCl_3$) to increase the tolerance coefficient of $CsPbI_2Br$. The results showed that the 0.4% $GdCl_3$-incorporated $CsPbI_2Br$ film had the highest PCE of 16.24%.

Since Eperon et al. [20] first prepared stable cubic $CsPbI_3$ films at room temperature by adding HI into its precursor solution, HI became the most common additive in $CsPbI_3$ PSCs. Some groups [70,71] suggested that the precursor solution with HI was a polar solvent, which could cause the α-$CsPbI_3$ to convert into the γ-$CsPbI_3$. Yu et al. [72] used 35 µL HI and 10 µL H_2O as additives to prepare high-quality $CsPbI_3$ films by one-step spin coating at 100 °C. In addition, the perovskite films containing micro-water had a smoother surface with bigger grain sizes. The grain interface was repaired by dissolution and recrystallization to obtain a smooth film after removing the water. The fill factor (FF) was increased from 62% to around 69% and the PCE was improved from 10.34% to 11.42%. However, some researchers reported that the water in the HI acid may give a passive effect to form perovskite. They used DMF instead of water. Zhang et al. [73] first used $HPbI_3$ to synthesize black $CsPbI_3$ perovskite films at 150 °C. Then, many groups added $HPbI_3$ in the precursor to prepare stable $CsPbI_3$ films [23,47,52,74–78]. The PSCs with the $HPbI_3$-treated $CsPbI_3$ have a PCE of over 18 % [48,78]. Xi et al. [79] found that adding more HI could get a new compound of H_2PbI_4. H_2PbI_4 could also increase the phase stability.

However, the mechanism of improving $CsPbI_3$ stability by $HPbI_3$ treatment is controversial. Some groups [80–82] found that the really useful material is $DMAPbI_3$, which was produced by the acid hydrolysis of DMF. DMA^+ has a bigger radius than Cs^+. When DMA^+ partially replaced Cs^+, it is easy to form a stable black phase. Some groups [78,83,84] had different opinions. They reported that annealing could remove most of the organic matter (DMA^+), so only $CsPbI_3$ was left. Some groups [29,85] even added DMAI into the $CsPbI_3$ precursor immediately and got the best PCE of 19.03% [29].

Adding precursor material itself into the perovskite is also a good choice. Xiang et al. [86] added extra CsI into the precursor solution to synthesize black $CsPbI_3$ films in an air atmosphere at 110 °C. Becker et al. [87] showed that more CsI in the precursor could directly obtain the γ-$CsPbI_3$ perovskite phase. Their CsI-rich device gave a PCE of 12.5%. Bai et al. [88] controlled the ratio of CsI and PbI_2 in the precursor precisely. The best PCE based on the obtained 0D Cs_4PbI_6 and γ-$CsPbI_3$ heterojunction was 16.39%. Fu et al. [89] introduced excess CsBr into the $CsPbI_3$ precursor to prepare a more stable $CsPbI_3$ phase at low temperatures.

Fu et al. [90] added 2-hydroxyethyl methacrylate (HEMA) into the perovskite precursor to simultaneously increase the crystallization and decrease the deficiencies. The performance was best when 3 mg/mL HEMA was added. Yoon et al. [91] controlled the crystal growth procedure by adding a methylammonium chloride SDMS solution in continuous drops. Then, they used octyl ammonium iodides to passivate the surface in ambient air. $CsPbI_3$ with a 45 mM MACl film was highly uniform and pinhole-minimized. Li et al. [92] introduced 16.90 $mg{\cdot}mL^{-1}$ $CsPbBr_3$ quantum dots on the surface of the $CsPbI_3$ film to passivate the deficiencies and improve the PCE to 16%. Zhang et al. [93] used the Zn^{2+} ions from zinc oxalate to recover the vacancies of Pb and Sn; then, they obtained perfect $CsPb_{0.7}Sn_{0.3}IBr_2$ films with high crystallinity and lower defect density. Wang et al. [94] improved the properties of $CsPbIBr_2$ films by bringing in a 3% molar ratio of guanidinium thiocyanate (GuaSCN), which was beneficial to optimize the PCE and stability of the PSCs. The various inorganic PSC performances using additive engineering are summarized in Table 1. Additive engineering was helpful for PSC performances. In addition to choosing the radius of the ions to add, the amount of material to add was also precisely controlled, as too many additions could have negative effects. Further, uncontrollable ionic components also greatly reduced the repeatability of the preparation process.

Table 1. Summary of various inorganic PSCs' performance using additive engineering.

Additive		Device Configuration	J_{sc} (mA cm^{-2})	V_{OC} (V)	FF	PCE (%)	Ref.
X site	Br^-	FTO/TiO_2/$CsPbI_2Br$/$CuBr_2$/Spiro-OMeTAD/MoO_3/Ag	16.95	1.18	0.8	16.15%	[9]
	Br^-	FTO/c-TiO_2/m-TiO_2/$CsPbI_2Br$/Spiro-OMeTAD/Ag	11.89	1.11	0.75	9.84	[25]
	Br^-	FTO/TiO_2/$CsPbI_{2.85}Br_{0.15}$/PTAA/Au	19.75	1.135	0.766	17.17	[47]
	Br^-	ITO/SnO_2/LiF/$CsPbI_{3-x}Br_x$/Spiro-OMeTAD/Au	18.3	1.25	0.825	18.64	[48]
	Br^-	ITO/SnO_2/$CsPbI_xBr_{3-x}$/SIM/Spiro-OMeTAD/Au	18.01	1.27	0.79	18.06	[49]
	Cl^-	FTO/TiO_2/γ-$CsPbI_3$:$Cl_{0.03}$/PTAA/Ag	19.58	1.084	0.757	16.07	[51]
	SCN^-	FTO/TiO_2/$CsPbI_3$/PTAA/Au	20.34	1.09	0.77	17.04	[52]
	SCN^-	ITO/TiO_2/$CsPbBr_3$-1.5% NH_4SCN/Spiro-OMeTAD/Au	7.76	1.375	0.793	8.47	[53]
B site	Sn^{2+}	FTO/c-TiO_2/$CsPbI_3$/CuSCN/Au	10.05	0.85	0.59	5.12	[55]
	Ca^{2+}	FTO/c-TiO_2/m-TiO_2/$CsPbI_3$/P3HT/Au	17.9	0.94	0.8	13.5	[56]
	Sr^{2+}	FTO/c-TiO_2/m-TiO_2/$CsPb_{0.98}Sr_{0.02}I_2Br$/P3HT/Au	15.3	1.043	0.699	11.2	[57]
	Ba^{2+}	ITO/SnO_2/$CsPbI_3$(α)/P3HT/Au	13.19	0.9	0.606	7.23	[59]
	Mn^{2+}	FTO/TiO_2/$CsPbI_3$/PTAA/Au	19.53	1.1	0.77	16.52	[62]
	Cd^{2+}	FTO/TiO_2/$CsPbIBr_2$-Cd^{2+}/Carbon	11.53	1.324	0.696	10.63	[63]
	Bi^{3+}	FTO/c-TiO_2/$CsPbI_3$(α)/CuI/Au	18.76	0.97	0.7259	13.21	[64]
	Sb^{3+}	FTO/c-TiO_2/$CsPbI_3$/Spiro-OMeTAD/Au	13.15	1.04	0.67	9.4	[65]
	Yb^{3+}	FTO/c-TiO_2/$CsPbI_3$(α)/Spiro-OMeTAD/Ag	18.4	1.13	0.6	12.4	[66]
	Eu^{3+}	FTO/TiO_2/$CsPbI_3$(α)/Spiro-OMeTAD/Au	11.1	0.898	0.68	6.8	[67]
	In^{3+}	FTO/c-TiO_2/m-TiO_2/$CsPbI_3$/Carbon	15.68	1.2	0.64	12.04	[18]
	Er^{3+}	ITO/NiO/CsI$(PbBr_2)_{0.97}$ $(ErCl_3)_{0.03}$/Nb_2O_5/Ag	12.36	1.34	0.705	11.61	[68]
	Gd^{3+}	FTO/TiO_2/$CsPbI_2Br_{0.96}$ $(GdCl_3)_{0.04}$/Spiro-OMeTAD/Au	16.09	1.222	0.825	16.24	[69]
HI		FTO/c-TiO_2/$CsPbI_3$ (γ)/P3HT/Au	16.53	1.04	0.657	11.3	[71]
$HPbI_3$		FTO/c-TiO_2/$CsPbI_3$ (α)/Spiro-OMeTAD/Ag	14.53	1.15	0.71	11.86	[73]
$HPbI_3$		FTO/c-TiO_2/m-TiO_2/$CsPbI_3$(α)/Carbon	18.5	0.79	0.65	9.5	[74]
$HPbI_3$		ITO/SnO_2/$CsPbI_3$/Spiro-OMeTAD/Au	16.59	1.07	0.7	12.4	[75]
$HPbI_3$		FTO/TiO_2/$CsPbI_3$(γ)/PTAA/Au	18.95	1.059	0.751	15.07	[76]
$HPbI_3$		FTO/c-TiO_2/$CsPbI_3$/Spiro-OMeTAD/Au	18.4	1.054	0.74	14.3	[77]
$HPbI_3$		FTO/c-TiO_2/$CsPbI_3$(α)/Spi ro-OMeTAD/Ag	18.76	1.104	0.806	17.06	[23]
$HPbI_3$		FTO/c-TiO_2/$CsPbI_3$(β)/Spiro-OMeTAD/Ag	20.23	1.11	0.82	18.4	[78]
H_2PbI_4		ITO/PTAA/$CsPbI_3$/ (C_{60}/BCP)/Cu	17.10	1.12	0.7	13.4	[79]
DMAI		FTO/PEDOT:PSS/CsPbI3/(C60/BCP)/Ag	16.65	0.99	0.765	12.62	[80]

Table 1. *Cont.*

Additive	Device Configuration	J_{sc} (mA cm^{-2})	V_{OC} (V)	FF	PCE (%)	Ref.
HI	FTO/c-TiO_2/$CsPbI_3$/ PTAA/Au	21.15	1.062	0.77	17.3	[83]
DMAI	FTO/c-TiO_2/m-TiO_2/$CsPbI_3$/Carbon	15.76	0.91	0.66	9.39	[84]
DMAI	FTO/c-TiO_2/$CsPbI_3$(β)/Spiro-OMeTAD/Ag	20.23	1.137	0.827	19.02	[29]
DMAI	FTO/c-TiO_2/m-TiO_2/$CsPbI_3$(γ)/Spiro-OMeTAD/Ag	19.4	1.05	0.75	15.3	[85]
CsI	FTO/c-TiO_2/m-TiO_2/m-Al_2O_3/$CsPbI_3$/Carbon	14.65	0.73	0.5	5.31	[86]
CsI	ITO/PTAA/$CsPbI_3$(γ)/C_{60}/BCP/Ag	17.8	0.96	0.73	12.5	[87]
CsI	ITO/SnO_2/ZnO/$CsPbI_3$/Spiro-OMeTAD/MoO_3/Ag	18.84	1.09	0.8	16.39	[88]
CsBr	FTO/ZnO/$CsPbI_{3-x}Br_x$)/Carbon	19.1	0.96	0.68	12.39	[89]
HEMA	FTO/ZnO/$CsPbI_2Br$/PM6/MoO_3/Ag	15.81	1.23	0.83	16.13	[90]
MACl	FTO/c-TiO_2/$CsPbI_3$/spiro-OMeTAD/Au	20.59	1.198	0.825	20.37	[91]
$CsPbBr_3$ QDs	ITO/SnO_2/$CsPbI_3$/$CsPbBr_3$ QDs/spiro-OMeTAD/Au	18.02	1.09	0.821	16.17	[92]
ZnOX	ITO/SnO_2/$CsPb_{1-x}Sn_xIBr_2$/Spiro-OMeTAD/Au	15.5	1.18	0.767	14.1	[93]
GuaSCN	FTO/c-TiO_2/$CsPbIBr_2$/Spiro-OMeTAD/Au	12.05	1.23	0.737	10.9	[94]

2.2. Solvent Engineering

Solvent engineering is a valid strategy to enhance the properties of perovskite for excellent PSCs [95]. Snaith et al. [25] prepared high-property $CsPbI_2Br$ film for the first time by precisely controlling the dissolvability of $CsPbI_2Br$ in DMF. McGehee et al. [27] used DMSO as the solvent to get high-property $CsPbI_2Br$ films. Some groups [57,96–99] used dimethyl sulfoxide (DMSO) and dimethyl formamide (DMF) as co-solvents to obtain a $CsPbI_2Br$ film, which could promote the solubility of $CsPbI_2Br$. Luo et al. [100] first obtained stable $CsPbI_3$ in fully open-air conditions by treating it with hydroiodic acid (HI) and isopropanol (IPA). Meng et al. [101] dissolved CsBr with ethylene glycol monomethyl ether (EGME) and IPA to control the Ostwald ripening. They got high crystalline and favorable $CsPbBr_3$ films. The EGME/IPA bi-solvent treatment increased the PCE from 3.57% to 7.29%.

With the increase of people's awareness of environmental protection, green solvents are becoming more and more popular. He et al. [102] proved that green antisolvent IPA and thiourea can optimize the quality of $CsPbIBr_2$ films. The carbon-based $CsPbIBr_2$ PSCs have a PCE of 6.79%, which was almost 30% higher than the untreated PSCs. Wang et al. [103] replaced the noxious methanol with the environmentally friendly bi-component solvent (water and ethylene glycol monomethyl ether) to prepare high-property $CsPbBr_3$ films. The $CsPbBr_3$ PSC showed an optimal PCE of 9.55% with remarkable humidity stability. The eco-friendly ethyl acetate (EA) is another kind of solvent used in solvent engineering. Dong et al. [104] showed that the green EA antisolvent can optimize the properties of the $CsPbI_2Br$ films. The EA-engineered $CsPbI_2Br$ helped the PCE reach 10.0%. Han et al. [105] showed that the green EA antisolvent was able to promote better growth of the $CsPbI_3$ films. Saparbaev et al. [106] used eco-friendly methylammonium acetate liquid to assemble $CsPbI_3$ PSCs with a PCE of 14.4%.

Regulating the preparation process with solvent engineering is also a valid method to optimize the quality of the all-inorganic perovskite films. Wang et al. [24] adopted a solvent-controlled growth method to obtain a stable α-$CsPbI_3$ film. The $CsPbI_3$ solar cells showed a 15.7% PCE. Teng et al. [107] reported that the decomposition rate of the $CsPbBr_3$ precursor in a CsBr and methanol solution was faster, and $CsPbBr_3$ films synthesized by the traditional two-step approach had low quality. Zai et al. [108] developed an easy low-temperature solution process to carefully regulate the $CsPbI_2Br$ crystallization kinetics, which increased PCE to 14.31%. The thermal and light stability was also perfect. Liu et al. [109] and Gao et al. [110] both applied a multistep spin-coating method to obtain the brilliant property of $CsPbBr_3$ films, which could improve the uniformity of nucleation. Wang et al. [111] found alcohol could cause a quick crystallization process of the $CsPbIBr_2$ films, which was very beneficial for improving its crystallinity. The obtained PSCs showed a high PCE of 11.49%. Wang et al. [112] adopted EAH-S solvent to extract the ammonium halide (Figure 2). This new strategy could solve the phase instability problems of $CsPbI_3$. The carbon-based $CsPbI_3$ PSCs attained a PCE of 15.35%. Zhong et al. [113] regulated the crystalline quality of $CsPbBr_3$ films by adding 2-phenethylamine bromide (PEABr) to the $PbBr_2$ DMF solution. The PCE increased to 8.25%. The PSCs' performances related to solvent engineering are summarized in Table 2.

Table 2. Summary of various inorganic PSCs' performance using solvent engineering.

Device Configuration	J_{sc} (mA cm^{-2})	V_{OC} (V)	FF (%)	PCE (%)	Ref.
ITO/PEDOT:PSS/$CsPbI_2Br$/PCBM/BCP/Al	10.9	1.06	-	6.8	[27]
FTO/NiOx/$CsPbI_2Br$/ZnO@C_{60}/Ag	15.2	1.14	0.77	13.3	[96]
ITO/c-TiO_2/$CsPbI_2Br$/Spiro-OMeTAD/Au	12.7	1.05	0.68	9.08	[97]
FTO/NiMgLiO/$CsPbI_2Br$/PCBM/BCP/Ag	14.18	0.98	0.66	9.14	[98]
FTO/TiO_2/$CsPbI_2Br$/Spiro-OMeTAD/Au	15.33	1.2	0.79	14.78	[99]
FTO/TiO_2/$CsPbI_3(\alpha)$/Spiro-MeOTAD/Ag	11.92	0.66	0.525	4.13	[100]
FTO/c-TiO_2/$CsPbBr_3$/Carbon	7.12	1.49	0.688	7.29	[101]
FTO/SnO_2/$CsPbIBr_2$/Carbon	10.15	1.19	0.563	6.79	[102]
FTO/c-TiO_2/$CsPbBr_3$/Carbon	7.48	1.51	0.845	9.55	[103]
FTO/c-TiO_2/$CsPbI_2Br$/Carbon	13.87	1.15	0.64	10.21	[104]
ITO/SnO_2/$CsPbI_3$/PEAI/Spiro-OMeTAD/MoO_3/Ag	19.43	0.737	0.615	8.8	[105]
ITO/PEDOT:PSS/$CsPbI_3$/PCBM/Al	18.66	1.05	0.733	14.4	[106]
ITO/SnO_2/$CsPbI_3$/Spiro-OMeTAD/Au	18.41	1.08	0.793	15.71	[24]
FTO/c-TiO_2/$CsPbBr_3$/carbon	6.46	1.34	0.68	5.86	[107]
ITO/SnO_2/$CsPbI_2Br$/PTAA/Au	14.6	1.162	0.791	14.31	[108]
FTO/Ni-TiO_2/SnO_2/$CsPbBr_3$/CuPc/Carbon	8.24	1.31	0.814	8.79	[109]
FTO/NiO_x/$CsPbBr_3$/$PC_{61}BM$/Ag	8.22	1.47	0.83	10.02	[110]
FTO/c-TiO_2/$CsPbIBr_2$/Spiro- OMeTAD/Ag	13.33	1.22	0.71	11.49	[111]
FTO/TiO_2/$CsPbI_3$/Carbon	18.7	1.075	0.764	15.35	[112]
FTO/TiO_2/$CsPbBr_3$/Carbon	8.51	1.31	-	8.25	[113]

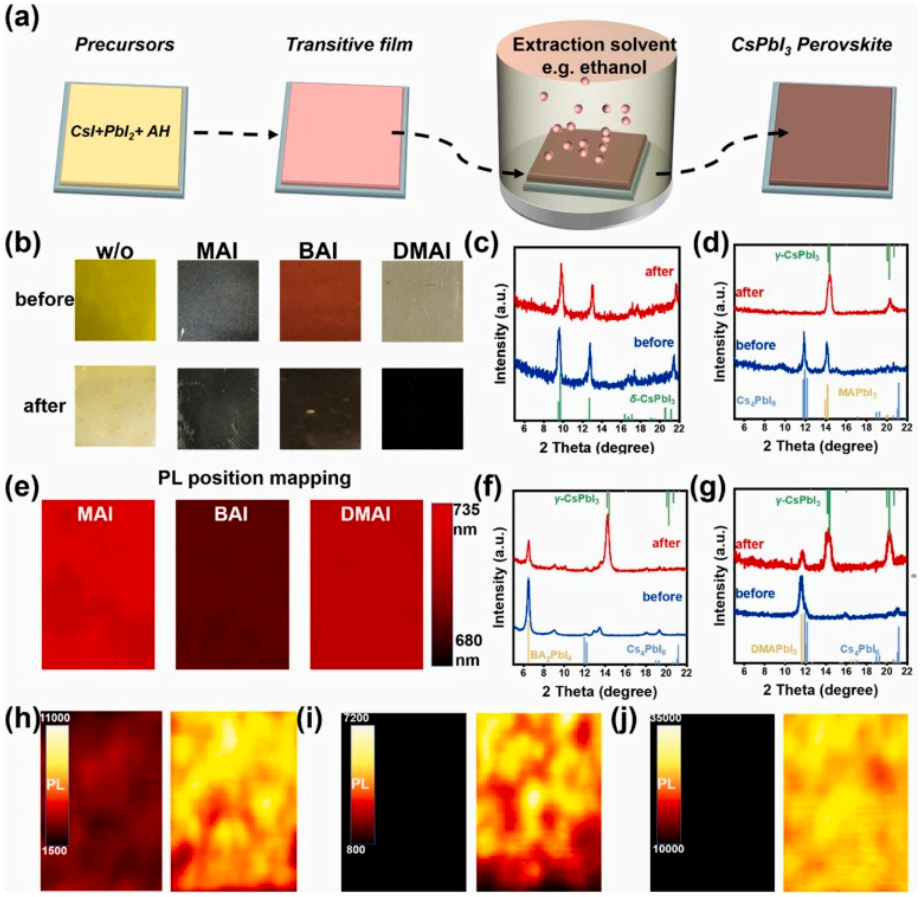

Figure 2. EAH-S method to grow $CsPbI_3$ perovskite. (**a**) Schematic diagram of EAH-S method. AH: ammonium halide. (**b**) Photographs of the transitive films prepared from the precursor solutions

with/without ammonium iodides and the corresponding films after soaking in EtOH. XRD patterns of the transitive films and the corresponding films after soaking in EtOH: (**c**) without ammonium iodides, (**d**) MAI, (**f**) BAI, and (**g**) DMAI. (**e**) PL position mapping of the transitive films after soaking in EtOH. PL intensity mapping of the transitive films and the corresponding films after soaking in EtOH: (**h**) MAI, (**i**) BAI, and (**j**) DMAI reprinted with permission from Ref. [112] 2022 Elsevier.

2.3. Interface Engineering

Interface engineering is also commonly used to modulate the morphology of perovskite films, stabilize the perovskite phase, and enhance operational stability [114,115]. Choosing contact materials and surface modification of the chosen contact materials are the main focuses of interface engineering research. For example, new materials are used in the electron transport layer (ETL). Yan et al. [116] introduced the SnO_2/ZnO bilayer ETL to obtain regular crystal grains and full coverage $CsPbI_2Br$ films. Yue et al. [117] used the ZnO-doped TiO_2 buffer layer to improve the PCE to 21.06%, and the V_{oc} and FF were 1.31 V and 74.1%. Yang et al. [118] explored a better wettability surface of the In_2S_3 ETL to increase the rate of $CsPbIBr_2$ nucleation. Zhu et al. [119] presented a TiO_2/SnO_2 ETL that could control the $CsPbIBr_2$ crystallization. Li et al. [120] adopted a strategy of interface engineering by depositing the $CsPbI_2Br$ perovskite film on a $ZnO/Mg_xZn_{1-x}O$ bilayer ETL, which could alleviate energy loss in the PSCs. The best PCE was 16.04%. Pan et al. [121] chose well-arranged TiO_2 nanopillar arrays (TiO_2 NaPAs) to boost the interface of $CsPbI_2Br$ and ETL, which resulted in continuously dense $CsPbI_2Br$ films, with few defects. Guo et al. [122] improved the perovskite quality by the passivation of SnO_2 ETL. It could enhance the carrier transport across the ETL/$CsPbIBr_2$ boundary surface, raise the charge reorganization resistance, and reduce the E_{loss} for the ultimate PSCs. Lu et al. [123] took $TiCl_4$ treatment to enhance the perovskite film property for better PSCs. The PCE of $TiCl_4$-TiO_2- and $TiCl_4$-ZnO-based PSCs increased to 16.5% and 17.0%, respectively. Wang et al. [124] adopted the amino group from polyethyleneimine ethoxylated (PEIE) to inactivate the defects of $CsPbIBr_2$ and increase the PCE from 8.7% to 11.2%. Wang et al. [125] modified the interface of TiO_2/perovskite with CsAc, which enhanced the $CsPbI_{2.25}Br_{0.75}$ film morphology, crystallinity, and electrochemical properties. The PSCs based on the CsAc-modified method showed an optimized PCE of 13.81%. Chai et al. [126] added $CsPbBr_3$ seeds into the TiO_2 ETL to regulate the $CsPbI_3$ crystal growth and promote the PCE (Figure 3). This new method provided a new idea for the commercial application of PSCs.

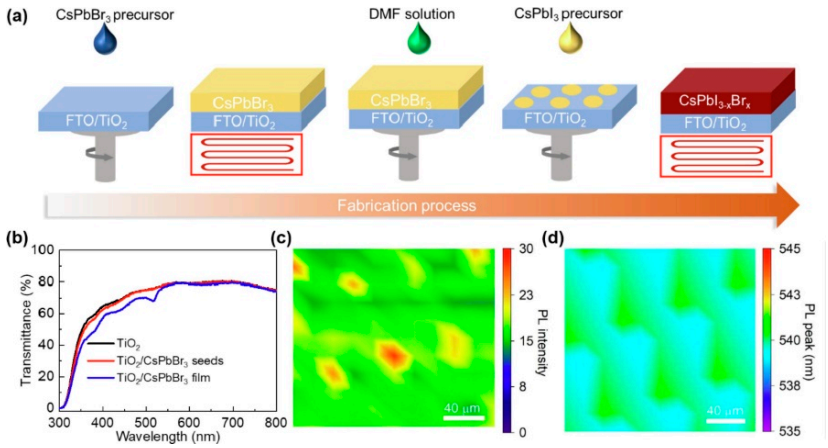

Figure 3. (**a**) Schematic of preparation process of $CsPbI_3$ films with $CsPbBr_3$ pieces. (**b**) Transmittance spectra of TiO_2, TiO_2/$CsPbBr_3$ seeds, and TiO_2/$CsPbBr_3$ film. (**c**) Confocal PL intensity and (**d**) PL peak position maps of TiO_2/$CsPbBr_3$ pieces, respectively reprinted with permission from Ref. [126] 2023 Elsevier.

The boundary surface between the perovskite and the hole transport layer (HTL) or electrode (without HTL) is another target to optimize perovskite film properties. Liu et al. [127] used a subtle MoOx cushion coat to raise the carrier injection, and reduce the trap state and the contact resistance. Zhou et al. [128] introduced an interfacial layer of MoO_3 to allow for highly competent charge separation and to suppress carrier reorganization. The PSCs exhibited a fairly high PCE of 14.05% with an FF of 81.5%. Zong et al. [129] introduced a simple synthetic and efficient MoO_2/N-doped carbon nanospheres complex inorganic HTL to establish a high capability and steady $CsPbBr_3$ PSCs. Xue et al. [130] used dopamine (DA) doping to improve the HTL work function and increase the perovskite film crystallinity. Ding et al. [131] modified a polyvinyl acetate with a carbonyl group at the boundary surface of $CsPbBr_3$/carbon to inactivate the perovskite surface defect states and intensify the energy level alignment between the $CsPbBr_3$ valence band and the carbon work function. Yang et al. [132] found that tris(N,N,N-tributyl-1-butanaminium)[[2,2′′6′,2′′-terpyridine] -4,4′,4 ′′—tricarboxylato(3−)-N1,N1′,N1′′]tris(thiocyanato-N)hydrogen ruthenate(4−) (N749) between the Cs-NiOx and $CsPbIBr_2$ can inhibit the phase separation and block moisture penetration. The inverted $CsPbIBr_2$ PSCs treated by N749 had amazing humidity stability. Zhu et al. [133] found that the diazonium atoms embracing the unpaired electrons in N,N′-Dicyclohexylcarbodiimide (DCC) have a strong passivation effect on the unpaired Pb^{2+} and Cs^+ ion drawbacks, which greatly reduced the drawback state of $CsPbBr_3$ films and caused the non-radiation reorganization. Du et al. [134] drafted (R)-(-)-1-cyclohexylethylamine iodide (R-CEAI) to inactivate the deficiencies of perovskite, and grew a quasi-2D Ruddlesden–Popper perovskite on the 3D perovskite. The R-CEAI-served 2D/3D PSCs had a PCE of 22.52%. Xu et al. [135] constructed a PbS/CdS heterojunction in $CsPbI_{1.5}Br_{1.5}$ and the carbon electrode to perfect the PSCs stability of the device. Zou et al. [136] passivated the $CsPbBr_3$/carbon interface by using NiO nanocrystals. The obtained $CsPbBr_3$ films showed prominent physical and chemical properties.

Some groups even considered both the perovskite/ETL and perovskite/HTL interfaces. Liao et al. [137] added carbon quantum dots to the $CsPbBr_3/TiO_2$ interfaces and red phosphorus quantum dots to the $CsPbBr_3$/Carbon interfaces, which accelerated both electron and hole transfer into the interface layer. As a result, the Voc was increased by about 0.2 V. $CsPbBr_3/CsSnBr_2I$ QDs bilayers [138], $CsPbBr_3$/CdZnSe@ZnSe QDs bilayers [139], and $CsPbI_2Br/CsPbI_3$ QDs bilayers [140] were also used to reduce the E_{loss}. Chen et al. [141] enhanced the morphology of $CsPbIBr_2$, PCE, and stability by introducing rubidium acetate (RbAc) to the ETL/perovskite/HTL interfaces. Shi et al. [142] synthesized two kinds of C_3N_4 materials (w-CN and y-CN) simultaneously and employed them in the two-sided boundary surface of the perovskite film. Table 3 summarizes the performances of PSCs based on interface engineering. The properties of the perovskite film were optimized, and the PCE was increased. Interface engineering can improve the transmission of charge between the interface of PSCs, reduce recombination loss, and improve the stability, which is an effective method to promote the photoelectric performance and long-term stability at the same time [143].

Table 3. Summary of various inorganic PSCs' performance using interface engineering.

Device Configuration	J_{sc} (mA cm^{-2})	V_{OC} (V)	FF (%)	PCE (%)	Ref.
ITO/SnO_2/ZnO/$CsPbI_2Br$/Spiro-OMeTAD/MoO_3/Ag	15	1.23	0.788	14.6	[116]
ITO/NiO_x/$CsPbI_3$/TiO_2/ZnO/Ag	21.79	1.31	0.741	21.06	[117]
ITO/In_2S_3/$CsPbIBr_2$/Sprio-OMeTAD/Au	7.76	1.09	0.66	5.59	[118]
FTO/SnO_2/TiO_2/CsBr/$CsPbIBr_2$/Carbon	10.91	1.273	0.66	9.31	[119]
ITO/ZnO/$Mg_xZn_{1-x}O$/$CsPbI_2Br$/PM6/MoO_3/Ag	15.8	1.31	0.78	16.04	[120]

Table 3. *Cont.*

Device Configuration	J_{sc} (mA cm^{-2})	V_{OC} (V)	FF (%)	PCE (%)	Ref.
ITO/TiO_2 CL@NaPA/$CsPbI_2Br$/P3HT/MoO_2/Ag	15.18	1.1	0.68	11.35	[121]
ITO/SnO_2/$CsPbIBr_2$/carbon	8.5	1.23	0.67	7	[122]
FTO/ZnO/$PC_{60}BM$/$CH_3NH_3PbI_{3-x}Cl_x$/spiro-OMeTAD/Ag	23.2	1.08	0.67	17	[123]
ITO/SnO_2/PEIE/$CsPbIBr_2$/Spiro-OMeTAD/MoO_3/Ag	11	1.29	0.786	11.2	[124]
FTO/CsAc@TiO_2 NRs/$CsPbI_{2.25}Br_{0.75}$/Carbon	16.29	1.145	0.741	13.81	[125]
FTO/TiO_2/$CsPbBr_3$ seeds//$CsPbI_3$/Spiro-OMeTAD/Ag	20.53	1.14	0.7946	18.6	[126]
FTO/NiOx/$CsPbIBr_2$/Au	10.44	0.62	0.52	3.4	[127]
ITO/SnO_2/$CsPbI_2Br$/Spiro-OMeTAD/MoO_3/Ag	15.4	1.12	0.815	14.05	[128]
FTO/c-TiO_2/m-TiO_2/$CsPbBr_3$/(MoO_2/NC)/Carbon	7.2	1.532	0.852	9.4	[129]
ITO/DA-PEDOT:PSS/perovskite/PCBM/PN4N/Ag	22	1.08	0.775	18.5	[130]
FTO/c-TiO_2/m-TiO_2/$CsPbBr_3$/PVAc/GO/Carbon	7.41	1.553	0.828	9.53	[131]
FTO/Cs-NiO_x/N749/$CsPbIBr_2$/$PC_{61}BM$/BCP/Ag	11.49	1.19	0.69	9.49	[132]
FTO/c-TiO_2/m-TiO_2/$CsPbBr_3$/DCC/Carbon	7.79	1.611	0.81	10.16	[133]
FTO/TiO_2/perovskite/R-CEAI/Spiro-OMeTAD/Au	23.42	1.195	0.805	22.52	[134]
FTO/TiO_2/$CsPbI_{1.5}Br_{1.5}$/PbS&R-CdS/Carbon	13.47	1.315	0.771	13.65	[135]
ITO/SnO_2/$CsPbBr_3$/NiO NCs/Carbon	7.57	1.57	0.774	9.19	[136]
FTO/c-TiO_2/m-TiO_2/$CsPbBr_3$/RPQD/Carbon	7.33	1.47	0.76	8.2	[137]
FTO/c-TiO_2/m-TiO_2/$CsPbBr_3$/$CsSnIBr_2$-QDs/Carbon	8.7	1.39	0.755	9.13	[138]
FTO/c-TiO_2/m-TiO_2/$CsPbBr_3$/QDs/Carbon	7.25	1.498	0.796	8.65	[139]
FTO/TiO_2/$CsPbI_2Br$/$CsPbI_3$-QDs/PTAA/Au	15.25	1.204	0.787	14.45	[140]
ITO/SnO_2/RbAc/$CsPbIBr_2$/RbAc/Spiro-OMeTAD/Ag	12.03	1.36	0.725	12.11	[141]
FTO/TiO_2/w-CN/$CsPbIBr_2$/y-CN	11.19	1.36	0.664	10.1	[142]

3. Results

Maximizing the PCE and improving the stability of all-inorganic $CsPbX_3$ perovskite solar cells is still a major challenge. We summarized some methods here. First, introducing additives such as X-site anions, B-site cations, HI, $HPbI_3$, precursor materials, and quantum dots could improve the crystallinity and morphology of the perovskite film. Choosing the appropriate radius for the addition was important, as was the molar ratio of the addition. Second, the proper solvent was helpful to enhance the properties of perovskite for excellent PSCs. To adapt to the future market demand, green solvents were popular. Third, interface modification could improve the film surface morphology and crystallinity. The charge transfer between layers was directly related to the PSCs' performance. The heterojunction will be one of the future trends. PCE, long-term stability, and preparation cost are important evaluation indices of solar cells. There is no doubt that all-inorganic PSCs have infinite potential and broad application prospects. However, compared with organic–inorganic hybrid PSCs, the PCE of all-inorganic PSCs still has a certain gap. Some existing problems and research prospects of all-inorganic PSCs are summarized as follows: (1) the mechanism of all-inorganic PSCs have not been studied thoroughly until now. It was difficult to optimize the PSCs' performance, ensure repeatability, and prepare them on a large scale. (2) There were inconsistencies in the evaluation of all-inorganic PSCs' stability in reports. It may be necessary in the future to develop uniform evaluation criteria to better adapt to commercial applications. (3) The toxicity of lead was an unavoidable problem and may be studied in terms of lead leakage or replacement.

Author Contributions: Conceptualization, Y.C. and F.L.; validation, Y.C., F.L., M.Z. and Z.Y.; writing—original draft preparation, Y.C. and F.L.; writing—review and editing, Y.C.; visualization, Y.C.; supervision, Y.C.; project administration, Y.C.; funding acquisition, Y.C. All authors have read and agreed to the published version of the manuscript.

Funding: This research was funded by the National Natural Science Foundation of China, grant number 21701041; the Open Foundation of Hubei Collaborative Innovation Center for High-Efficiency Utilization of Solar Energy, grant number HBSKFQN2017001; and the Talents of the High-Level Scientific Research Foundation of the Hubei University of Technology, grant number BSQD2017010.

Institutional Review Board Statement: Not applicable.

Informed Consent Statement: Not applicable.

Data Availability Statement: No new data were created or analyzed in this study. Data sharing is available within the article.

Conflicts of Interest: The authors declare no conflict of interest.

References

1. Xu, L.; Yuan, S.; Ma, L.; Zhang, B.; Fang, T.; Li, X.; Song, J. All-inorganic perovskite quantum dots as light-harvesting, interfacial, and light-converting layers toward solar cells. *J. Mater. Chem. A* **2021**, *9*, 18947–18973. [CrossRef]
2. Xiang, W.; Tress, W. Review on Recent Progress of All-Inorganic Metal Halide Perovskites and Solar Cells. *Adv. Mater.* **2019**, *31*, 1902851. [CrossRef]
3. Zhou, N.; Zhou, H. Spacer Organic Cation Engineering for Quasi-2D Metal Halide Perovskites and the Optoelectronic Application. *Small Struct.* **2022**, *3*, 2100232. [CrossRef]
4. Zhu, W.K.; Wang, S.R.; Zhang, X.; Wang, A.L.; Wu, C.; Hao, F. Ion Migration in Organic-Inorganic Hybrid Perovskite Solar Cells: Current Understanding and Perspectives. *Small* **2022**, *18*, 2105783. [CrossRef]
5. Ghosh, P.; Bruckbauer, J.; Trager-Cowan, C.; Krishnan Jagadamma, L. Crystalline grain engineered $CsPbIBr_2$ films for indoor photovoltaics. *Appl. Surf. Sci.* **2022**, *592*, 152865. [CrossRef]
6. Wu, T.; Qin, Z.; Wang, Y.; Wu, Y.; Chen, W.; Zhang, S.; Cai, M.; Dai, S.; Zhang, J.; Liu, J.; et al. The Main Progress of Perovskite Solar Cells in 2020–2021. *Nano Micro Lett.* **2021**, *13*, 152. [CrossRef]
7. Lai, C.S.; Jia, Y.; Lai, L.L.; Xu, Z.; McCulloch, M.D.; Wong, K.P. A comprehensive review on large-scale photovoltaic system with applications of electrical energy storage. *Renew. Sustain.Energy Rev.* **2017**, *78*, 439–451. [CrossRef]
8. Ma, X.; Yang, L.; Zheng, S.; Dai, Q.; Chen, C.; Song, H. All-Inorganic Perovskite Solar Cells: Status and Future. *Prog. Chem.* **2020**, *32*, 1608–1632. [CrossRef]
9. Wang, K.L.; Wang, R.; Wang, Z.K.; Li, M.; Zhang, Y.; Ma, H.; Liao, L.S.; Yang, Y. Tailored Phase Transformation of $CsPbI_2Br$ Films by Copper(II) Bromide for High-Performance All-Inorganic Perovskite Solar Cells. *Nano Lett.* **2019**, *19*, 5176–5184. [CrossRef]
10. Yao, X.; He, B.; Zhu, J.; Ti, J.; Cui, L.; Tui, R.; Wei, M.; Chen, H.; Duan, J.; Duan, Y.; et al. Tailoring type-II all-in-one buried interface for 1.635V-voltage, all-inorganic $CsPbBr_3$ perovskite solar cells. *Nano Energy* **2022**, *96*, 107138. [CrossRef]
11. Faheem, M.B.; Khan, B.; Feng, C.; Farooq, M.U.; Raziq, F.; Xiao, Y.; Li, Y. All-Inorganic Perovskite Solar Cells: Energetics, Key Challenges, and Strategies toward Commercialization. *ACS Energy Lett.* **2020**, *5*, 290–320. [CrossRef]
12. Yoo, J.J.; Seo, G.; Chua, M.R.; Park, T.G.; Lu, Y.; Rotermund, F.; Kim, Y.-K.; Moon, C.S.; Jeon, N.J.; Correa-Baena, J.-P.; et al. Efficient perovskite solar cells via improved carrier management. *Nature* **2021**, *590*, 587–593. [CrossRef] [PubMed]
13. Jena, A.K.; Kulkarni, A.; Miyasaka, T. Halide Perovskite Photovoltaics: Background, Status, and Future Prospects. *Chem. Rev.* **2019**, *119*, 3036–3103. [CrossRef]
14. Zhang, D.; Yuan, J.F.; Tian, J.J. All-inorganic perovskite solar cells with efficiency >20%. *Sci. China Mater.* **2021**, *64*, 2624–2626. [CrossRef]
15. Dong, C.; Xu, B.; Liu, D.; Moloney, E.G.; Tan, F.; Yue, G.; Liu, R.; Zhang, D.; Zhang, W.; Saidaminov, M.I. Carbon-based all-inorganic perovskite solar cells: Progress, challenges and strategies toward 20% efficiency. *Mater. Today* **2021**, *50*, 239–258. [CrossRef]
16. Maafa, I.M. All-Inorganic Perovskite Solar Cells: Recent Advancements and Challenges. *Nanomaterials* **2022**, *12*, 1651. [CrossRef]
17. Brunetti, B.; Cavallo, C.; Ciccioli, A.; Gigli, G.; Latini, A. On the Thermal and Thermodynamic (In)Stability of Methylammonium Lead Halide Perovskites. *Sci. Rep.* **2016**, *6*, 31896. [CrossRef]
18. Liang, J.; Han, X.; Yang, J.H.; Zhang, B.Y.; Fang, Q.Y.; Zhang, J.; Ai, Q.; Ogle, M.M.; Terlier, T.; Marti, A.A.; et al. Defect-Engineering-Enabled High-Efficiency All-Inorganic Perovskite Solar Cells. *Adv. Mater.* **2019**, *31*, 1903448. [CrossRef]
19. Juarez-Perez, E.J.; Ono, L.K.; Maeda, M.; Jiang, Y.; Hawash, Z.; Qi, Y. Photodecomposition and thermal decomposition in methylammonium halide lead perovskites and inferred design principles to increase photovoltaic device stability. *J. Mater. Chem. A* **2018**, *6*, 9604–9612. [CrossRef]
20. Eperon, G.E.; Paterno, G.M.; Sutton, R.J.; Zampetti, A.; Haghighirad, A.A.; Cacialli, F.; Snaith, H.J. Inorganic caesium lead iodide perovskite solar cells. *J. Mater. Chem. A* **2015**, *3*, 19688–19695. [CrossRef]
21. Liu, X.; Chen, M.; Zhang, Y.; Xia, J.; Yin, J.; Li, M.; Brooks, K.G.; Hu, R.; Gao, X.; Kim, Y.H.; et al. High-efficiency perovskite photovoltaic modules achieved via cesium doping. *Chem. Eng. J.* **2022**, *431*, 133713. [CrossRef]
22. Steele, J.A.; Jin, H.; Dovgaliuk, I.; Berger, R.F.; Braeckevelt, T.; Yuan, H.; Martin, C.; Solano, E.; Lejaeghere, K.; Rogge, S.M.J.; et al. Thermal unequilibrium of strained black $CsPbI_3$ thin films. *Science* **2019**, *365*, 679–684. [CrossRef]
23. Wang, Y.; Zhang, T.; Kan, M.; Zhao, Y. Bifunctional Stabilization of All-Inorganic alpha-$CsPbI_3$ Perovskite for 17% Efficiency Photovoltaics. *J. Am. Chem. Soc.* **2018**, *140*, 12345–12348. [CrossRef] [PubMed]
24. Wang, P.; Zhang, X.; Zhou, Y.; Jiang, Q.; Ye, Q.; Chu, Z.; Li, X.; Yang, X.; Yin, Z.; You, J. Solvent-controlled growth of inorganic perovskite films in dry environment for efficient and stable solar cells. *Nat. Commun.* **2018**, *9*, 2225. [CrossRef] [PubMed]

25. Sutton, R.J.; Eperon, G.E.; Miranda, L.; Parrott, E.S.; Kamino, B.A.; Patel, J.B.; Horantner, M.T.; Johnston, M.B.; Haghighirad, A.A.; Moore, D.T.; et al. Bandgap-Tunable Cesium Lead Halide Perovskites with High Thermal Stability for Efficient Solar Cells. *Adv. Energy Mater.* **2016**, *6*, 1502458. [CrossRef]
26. Ahmad, W.; Khan, J.; Niu, G.; Tang, J. Inorganic $CsPbI_3$ Perovskite-Based Solar Cells: A Choice for a Tandem Device. *Sol. RRL* **2017**, *1*, 1700048. [CrossRef]
27. Beal, R.E.; Slotcavage, D.J.; Leijtens, T.; Bowring, A.R.; Belisle, R.A.; Nguyen, W.H.; Burkhard, G.F.; Hoke, E.T.; McGehee, M.D. Cesium Lead Halide Perovskites with Improved Stability for Tandem Solar Cells. *J. Phys. Chem. Lett.* **2016**, *7*, 746–751. [CrossRef]
28. Ding, X.; Chen, H.; Wu, Y.; Ma, S.; Dai, S.; Yang, S.; Zhu, J. Triple cation additive $NH^{3+}C_2H_4NH^{2+}C_2H_4NH^{3+}$-induced phase-stable inorganic α-$CsPbI_3$ perovskite films for use in solar cells. *J. Mater. Chem. A* **2018**, *6*, 18258–18266. [CrossRef]
29. Wang, Y.; Liu, X.; Zhang, T.; Wang, X.; Kan, M.; Shi, J.; Zhao, Y. The Role of Dimethylammonium Iodide in $CsPbI_3$ Perovskite Fabrication: Additive or Dopant? *Angew. Chem. Int. Ed.* **2019**, *58*, 16691–16696. [CrossRef]
30. Yang, S.; Duan, Y.; Liu, Z.; Liu, S. Recent Advances in $CsPbX_3$ Perovskite Solar Cells: Focus on Crystallization Characteristics and Controlling Strategies. *Adv. Energy Mater.* **2022**, *2201733*. [CrossRef]
31. Wang, L.; Fan, B.; Zheng, B.; Yang, Z.; Yin, P.; Huo, L. Organic functional materials: Recent advances in all-inorganic perovskite solar cells. *Sustain. Energy Fuels* **2020**, *4*, 2134–2148. [CrossRef]
32. Duan, J.; Xu, H.; Sha, W.E.I.; Zhao, Y.; Wang, Y.; Yang, X.; Tang, Q. Inorganic perovskite solar cells: An emerging member of the photovoltaic community. *J. Mater. Chem. A* **2019**, *7*, 21036–21068. [CrossRef]
33. Yu, P.; Zhang, W.; Ren, F.; Wang, J.; Wang, H.; Chen, R.; Zhang, S.; Zhang, Y.; Liu, Z.; Chen, W. Strategies for highly efficient and stable cesium lead iodide perovskite photovoltaics: Mechanisms and processes. *J. Mater. Chem. C* **2022**, *10*, 4999–5023. [CrossRef]
34. Ullah, S.; Wang, J.M.; Yang, P.X.; Liu, L.L.; Yang, S.E.; Xia, T.Y.; Guo, H.Z.; Chen, Y.S. All-inorganic $CsPbBr_3$ perovskite: A promising choice for photovoltaics. *Mater. Adv.* **2021**, *2*, 646–683. [CrossRef]
35. Tai, Q.; Tang, K.-C.; Yan, F. Recent progress of inorganic perovskite solar cells. *Energy Environ. Sci.* **2019**, *12*, 2375–2405. [CrossRef]
36. Duan, C.P.; Zhao, Z.C.; Yuan, L.J. Lead-Free Cesium-Containing Halide Perovskite and Its Application in Solar Cells. *IEEE J. Photovol.* **2021**, *11*, 1126–1135. [CrossRef]
37. Wu, H.; Pi, J.; Zhou, D.; Wang, Q.; Long, Z.; Qiu, J. Effect of cation vacancy on lattice and luminescence properties in $CsPbBr_3$ quantum dots. *Ceram. Int.* **2022**, *48*, 3383–3389. [CrossRef]
38. Aftab, A.; Ahmad, M.I. A review of stability and progress in tin halide perovskite solar cell. *Sol. Energy* **2021**, *216*, 26–47. [CrossRef]
39. Marronnier, A.; Roma, G.; Boyer-Richard, S.; Pedesseau, L.; Jancu, J.-M.; Bonnassieux, Y.; Katan, C.; Stoumpos, C.C.; Kanatzidis, M.G.; Even, J. Anharmonicity and Disorder in the Black Phases of Cesium Lead Iodide Used for Stable Inorganic Perovskite Solar Cells. *ACS Nano* **2018**, *12*, 3477–3486. [CrossRef]
40. Montecucco, R.; Quadrivi, E.; Po, R.; Grancini, G. All-Inorganic Cesium-Based Hybrid Perovskites for Efficient and Stable Solar Cells and Modules. *Adv. Energy Mater.* **2021**, *11*, 2100672. [CrossRef]
41. Ahmed, Y.; Khan, B.; Faheem, M.B.; Huang, K.Q.; Gao, Y.J.; Yang, J.L. Organic additives in all-inorganic perovskite solar cells and modules: From moisture endurance to enhanced efficiency and operational stability. *J. Energy Chem.* **2022**, *67*, 361–390. [CrossRef]
42. Deng, J.; Li, J.; Yang, Z.; Wang, M. All-inorganic lead halide perovskites: A promising choice for photovoltaics and detectors. *J. Mater. Chem. C* **2019**, *7*, 12415–12440. [CrossRef]
43. Bensouda, Y.; Barrit, D. Mini-review on all-inorganic lead-based perovskite solar cells: Challenges and opportunities for production and upscaling. *Emergent Mater.* **2022**, *5*, 207–225. [CrossRef]
44. Ouedraogo, N.A.N.; Chen, Y.; Xiao, Y.Y.; Meng, Q.; Han, C.B.; Yan, H.; Zhang, Y. Stability of all-inorganic perovskite solar cells. *Nano Energy* **2020**, *67*, 104249. [CrossRef]
45. Zhang, C.L.; Arumugam, G.M.; Liu, C.; Hu, J.L.; Yang, Y.Z.; Schropp, R.E.I.; Mai, Y.H. Inorganic halide perovskite materials and solar cells. *APL Mater.* **2019**, *7*, 120702. [CrossRef]
46. Dastidar, S.; Egger, D.A.; Tan, L.Z.; Cromer, S.B.; Dillon, A.D.; Liu, S.; Kronik, L.; Rappe, A.M.; Fafarman, A.T. High Chloride Doping Levels Stabilize the Perovskite Phase of Cesium Lead Iodide. *Nano Lett.* **2016**, *16*, 3563–3570. [CrossRef]
47. Wang, H.; Bian, H.; Jin, Z.; Zhang, H.; Liang, L.; Wen, J.; Wang, Q.; Ding, L.; Liu, S.F. Cesium Lead Mixed-Halide Perovskites for Low-Energy Loss Solar Cells with Efficiency Beyond 17%. *Chem. Mater.* **2019**, *31*, 6231–6238. [CrossRef]
48. Ye, Q.; Zhao, Y.; Mu, S.; Ma, F.; Gao, F.; Chu, Z.; Yin, Z.; Gao, P.; Zhang, X.; You, J. Cesium Lead Inorganic Solar Cell with Efficiency beyond 18% via Reduced Charge Recombination. *Adv. Mater.* **2019**, *31*, e1905143. [CrossRef]
49. Zheng, Y.F.; Yang, X.Y.; Su, R.; Wu, P.; Gong, Q.H.; Zhu, R. High-Performance $CsPbI_xBr_{3-x}$ All-Inorganic Perovskite Solar Cells with Efficiency over 18% via Spontaneous Interfacial Manipulation. *Adv. Funct. Mater.* **2020**, *30*, 2000457. [CrossRef]
50. Ke, W.; Yang, X.; Liu, T. Resistance Switching Effect of Memory Device Based on All-Inorganic $Cspbbri_2$ Perovskite. *Materials* **2021**, *14*, 6629. [CrossRef]
51. Wang, K.; Jin, Z.; Liang, L.; Bian, H.; Wang, H.; Feng, J.; Wang, Q.; Liu, S. Chlorine doping for black gamma-$CsPbI_3$ solar cells with stabilized efficiency beyond 16%. *Nano Energy* **2019**, *58*, 175–182. [CrossRef]
52. Yao, Z.; Jin, Z.W.; Zhang, X.R.; Wang, Q.; Zhang, H.; Xu, Z.; Ding, L.M.; Liu, S.Z. Pseudohalide (SCN^-)-doped $CsPbI_3$ for high-performance solar cells. *J. Mater. Chem. C* **2019**, *7*, 13736–13742. [CrossRef]
53. Wang, D.; Li, W.J.; Du, Z.B.; Li, G.D.; Sun, W.H.; Wu, J.H.; Lan, Z. Highly Efficient $CsPbBr_3$ Planar Perovskite Solar Cells via Additive Engineering with NH_4SCN. *ACS Appl. Mater. Interfaces* **2020**, *12*, 10579–10587. [CrossRef] [PubMed]

54. Swarnkar, A.; Mir, W.J.; Nag, A. Can B-Site Doping or Alloying Improve Thermal- and Phase-Stability of All-Inorganic $CsPbX_3$ (X = Cl, Br, I) Perovskites? *ACS Energy Lett.* **2018**, *3*, 286–289. [CrossRef]
55. Murugadoss, G.; Thangamuthu, R. Metals doped cesium based all inorganic perovskite solar cells: Investigations on Structural, morphological and optical properties. *Sol. Energy* **2019**, *179*, 151–163. [CrossRef]
56. Lau, C.F.J.; Deng, X.; Zheng, J.; Kim, J.; Zhang, Z.; Zhang, M.; Bing, J.; Wilkinson, B.; Hu, L.; Patterson, R.; et al. Enhanced performance via partial lead replacement with calcium for a $CsPbI_3$ perovskite solar cell exceeding 13% power conversion efficiency. *J. Mater. Chem. A* **2018**, *6*, 5580–5586. [CrossRef]
57. Lau, C.F.J.; Zhang, M.; Deng, X.; Zheng, J.; Bing, J.; Ma, Q.; Kim, J.; Hu, L.; Green, M.A.; Huang, S.; et al. Strontium-Doped Low-Temperature-Processed $CsPbI_2Br$ Perovskite Solar Cells. *ACS Energy Lett.* **2017**, *2*, 2319–2325. [CrossRef]
58. Xue-Ting, W.; Yu-Hao, F.; Guang-Ren, N.; Hong-Dong, L.; Li-Jun, Z. Barium as doping element tuning both toxicity and optoelectric properties of lead-based halide perovskites. *Acta Phys. Sin.* **2019**, *68*, 157101. [CrossRef]
59. Kajal, S.; Kim, G.-H.; Myung, C.W.; Shin, Y.S.; Kim, J.; Jeong, J.; Jana, A.; Kim, J.Y.; Kim, K.S. A thermally stable, barium-stabilized α-$CsPbI_3$ perovskite for optoelectronic devices. *J. Mater. Chem. A* **2019**, *7*, 21740–21746. [CrossRef]
60. Zou, S.; Liu, Y.; Li, J.; Liu, C.; Feng, R.; Jiang, F.; Li, Y.; Song, J.; Zeng, H.; Hong, M.; et al. Stabilizing Cesium Lead Halide Perovskite Lattice through Mn(II) Substitution for Air-Stable Light-Emitting Diodes. *J. Am. Chem. Soc.* **2017**, *139*, 11443–11450. [CrossRef]
61. Akkerman, Q.A.; Meggiolaro, D.; Dang, Z.; De Angelis, F.; Manna, L. Fluorescent Alloy $CsPb_xMn_{1-x}I_3$ Perovskite Nanocrystals with High Structural and Optical Stability. *ACS Energy Lett.* **2017**, *2*, 2183–2186. [CrossRef] [PubMed]
62. Yao, Z.; Zhao, W.; Chen, S.; Jin, Z.; Liu, S.F. Mn Doping of $CsPbI_3$ Film Towards High-Efficiency Solar Cell. *ACS Appl. Energy Mater.* **2020**, *3*, 5190–5197. [CrossRef]
63. Xu, Y.; Li, G.D.; Jing, Y.; Zhang, H.Y.; Wang, X.; Lu, Y.; Wu, J.H.; Lan, Z. n-type absorber by Cd^{2+} doping achieves high-performance carbon-based $CsPbIBr_2$ perovskite solar cells. *J. Colloid Interface Sci.* **2022**, *608*, 40–47. [CrossRef] [PubMed]
64. Hu, Y.; Bai, F.; Liu, X.; Ji, Q.; Miao, X.; Qiu, T.; Zhang, S. Bismuth Incorporation Stabilized alpha-$CsPbI_3$ for Fully Inorganic Perovskite Solar Cells. *ACS Energy Lett.* **2017**, *2*, 2219–2227. [CrossRef]
65. Bera, S.; Ghosh, D.; Dutta, A.; Bhattacharyya, S.; Chakraborty, S.; Pradhan, N. Limiting Heterovalent B-Site Doping in $CsPbI_3$ Nanocrystals: Phase and Optical Stability. *ACS Energy Lett.* **2019**, *4*, 1364–1369. [CrossRef]
66. Wang, M.; Deng, K.M.; Meng, L.X.; Li, L. Bifunctional Ytterbium (III) Chloride Driven Low-Temperature Synthesis of Stable alpha-$CsPbI_3$ for High-Efficiency Inorganic Perovskite Solar Cells. *Small Methods* **2020**, *4*, 1900652. [CrossRef]
67. Jena, A.K.; Kulkarni, A.; Sanehira, Y.; Ikegami, M.; Miyasaka, T. Stabilization of alpha-$CsPbI_3$ in Ambient Room Temperature Conditions by Incorporating Eu into $CsPbI_3$. *Chem. Mater.* **2018**, *30*, 6668–6674. [CrossRef]
68. Faheem, M.B.; Khan, B.; Feng, C.; Ahmed, S.B.; Jiang, J.X.; Rehman, M.U.; Subhani, W.S.; Farooq, M.U.; Nie, J.L.; Makhlouf, M.M.; et al. Synergistic Approach toward Erbium-Passivated Triple-Anion Organic-Free Perovskite Solar Cells with Excellent Performance for Agrivoltaics Application. *ACS Appl. Mater. Interfaces* **2022**, *14*, 6894–6905. [CrossRef]
69. Pu, X.; Yang, J.; Wang, T.; Cheng, S.; Cao, Q.; Zhao, J.; Chen, H.; Zhang, Y.; Xu, T.; Tojiboyev, I.; et al. Gadolinium-incorporated $CsPbI_2Br$ for boosting efficiency and long-term stability of all-inorganic perovskite solar cells. *J. Energy Chem.* **2022**, *70*, 9–17. [CrossRef]
70. Sun, J.-K.; Huang, S.; Liu, X.-Z.; Xu, Q.; Zhang, Q.-H.; Jiang, W.-J.; Xue, D.-J.; Xu, J.-C.; Ma, J.-Y.; Ding, J.; et al. Polar Solvent Induced Lattice Distortion of Cubic $CsPbI_3$ Nanocubes and Hierarchical Self-Assembly into Orthorhombic Single-Crystalline Nanowires. *J. Am. Chem. Soc.* **2018**, *140*, 11705–11715. [CrossRef]
71. Zhao, B.Y.; Jin, S.F.; Huang, S.; Liu, N.; Ma, J.Y.; Xue, D.J.; Han, Q.W.; Ding, J.; Ge, Q.Q.; Feng, Y.Q.; et al. Thermodynamically Stable Orthorhombic gamma-$CsPbI_3$ Thin Films for High-Performance Photovoltaics. *J. Am. Chem. Soc.* **2018**, *140*, 11716–11725. [CrossRef] [PubMed]
72. Gao, Y.; Xu, W.; He, F.; Fan, T.; Cai, W.; Zhang, X.; Wei, G. Boosting Performance of $CsPbI_3$ Perovskite Solar Cells via the Synergy of Hydroiodic Acid and Deionized Water. *Adv. Energy Sustain. Res.* **2022**, *3*, 2100149. [CrossRef]
73. Zhang, T.; Dar, M.I.; Li, G.; Xu, F.; Guo, N.; Gratzel, M.; Zhao, Y. Bication lead iodide 2D perovskite component to stabilize inorganic alpha-$CsPbI_3$ perovskite phase for high-efficiency solar cells. *Sci. Adv.* **2017**, *3*, 1700841. [CrossRef]
74. Xiang, S.; Fu, Z.; Li, W.; Wei, Y.; Liu, J.; Liu, H.; Zhu, L.; Zhang, R.; Chen, H. Highly Air-Stable Carbon-Based α-$CsPbI_3$ Perovskite Solar Cells with a Broadened Optical Spectrum. *ACS Energy Lett.* **2018**, *3*, 1824–1831. [CrossRef]
75. Jiang, Y.; Yuan, J.; Ni, Y.; Yang, J.; Wang, Y.; Jiu, T.; Yuan, M.; Chen, J. Reduced-Dimensional alpha-$CsPbX_3$ Perovskites for Efficient and Stable Photovoltaics. *Joule* **2018**, *2*, 1356–1368. [CrossRef]
76. Wang, K.; Jin, Z.; Liang, L.; Bian, H.; Bai, D.; Wang, H.; Zhang, J.; Wang, Q.; Liu, S. All-inorganic cesium lead iodide perovskite solar cells with stabilized efficiency beyond 15%. *Nat. Commun.* **2018**, *9*, 4544. [CrossRef] [PubMed]
77. Pei, Y.H.; Liu, Y.; Li, F.M.; Bai, S.; Jian, X.; Liu, M.Z. Unveiling Property of Hydrolysis-Derived $DMAPbI_{(3)}$ for Perovskite Devices: Composition Engineering, Defect Mitigation, and Stability Optimization. *iScience* **2019**, *15*, 165–172. [CrossRef] [PubMed]
78. Wang, Y.; Dar, M.I.; Ono, L.K.; Zhang, T.; Kan, M.; Li, Y.; Zhang, L.; Wang, X.; Yang, Y.; Gao, X.; et al. Thermodynamically stabilized beta-$CsPbI_3$-based perovskite solar cells with efficiencies >18%. *Science* **2019**, *365*, 591–595. [CrossRef]
79. Xi, J.; Piao, C.; Byeon, J.; Yoon, J.; Wu, Z.; Choi, M. Rational Core–Shell Design of Open Air Low Temperature In Situ Processable $CsPbI_3$ Quasi-Nanocrystals for Stabilized p-i-n Solar Cells. *Adv. Energy Mater.* **2019**, *9*, 1901787. [CrossRef]

80. Ke, W.J.; Spanopoulos, I.; Stoumpos, C.C.; Kanatzidis, M.G. Myths and reality of $HPbI_3$ in halide perovskite solar cells. *Nat. Commun.* **2018**, *9*, 4785. [CrossRef]
81. Daub, M.; Hillebrecht, H. On the Demystification of "$HPbI_3$" and the Peculiarities of the Non-innocent Solvents H_2O and DMF. *Z. Anorg. Allg. Chem* **2018**, *644*, 1393–1400. [CrossRef]
82. Zhang, J.; Yang, L.; Zhong, Y.; Hao, H.; Yang, M.; Liu, R. Improved phase stability of the $CsPbI_3$ perovskite via organic cation doping. *Phys. Chem. Chem. Phys.* **2019**, *21*, 11175–11180. [CrossRef] [PubMed]
83. Bian, H.; Wang, H.; Li, Z.; Zhou, F.; Xu, Y.; Zhang, H.; Wang, Q.; Ding, L.; Liu, S.; Jin, Z. Unveiling the Effects of Hydrolysis-Derived $DMAI/DMAPbI_{(x)}$ Intermediate Compound on the Performance of $CsPbI_3$ Solar Cells. *Adv. Sci.* **2020**, *7*, 1902868. [CrossRef] [PubMed]
84. Wang, H.L.; Xiang, S.S.; Li, W.P.; Liu, H.C.; Zhu, L.Q.; Xiao, S.; Yang, S.H.; Chen, H.N. Skillfully deflecting the question: A small amount of piperazine-1,4-diium iodide radically enhances the thermal stability of $CsPbI_3$ perovskite. *J. Mater. Chem. C* **2019**, *7*, 11757–11763. [CrossRef]
85. Meng, H.G.; Shao, Z.P.; Wang, L.; Li, Z.P.; Liu, R.R.; Fan, Y.P.; Cui, G.L.; Pang, S.P. Chemical Composition and Phase Evolution in DMAI-Derived Inorganic Perovskite Solar Cells. *ACS Energy Lett.* **2020**, *5*, 263–270. [CrossRef]
86. Xiang, S.; Li, W.; Wei, Y.; Liu, J.; Liu, H.; Zhu, L.; Chen, H. The synergistic effect of non-stoichiometry and Sb-doping on air-stable alpha-$CsPbI_3$ for efficient carbon-based perovskite solar cells. *Nanoscale* **2018**, *10*, 9996–10004. [CrossRef]
87. Becker, P.; Márquez, J.A.; Just, J.; Al-Ashouri, A.; Hages, C.; Hempel, H.; Jošt, M.; Albrecht, S.; Frahm, R.; Unold, T. Low Temperature Synthesis of Stable γ-$CsPbI_3$ Perovskite Layers for Solar Cells Obtained by High Throughput Experimentation. *Adv. Energy Mater.* **2019**, *9*, 1900555. [CrossRef]
88. Bai, F.J.; Zhang, J.; Yuan, Y.F.; Liu, H.B.; Li, X.S.; Chueh, C.C.; Yan, H.; Zhu, Z.L.; Jen, A.K.Y. A 0D/3D Heterostructured All-Inorganic Halide Perovskite Solar Cell with High Performance and Enhanced Phase Stability. *Adv. Mater.* **2019**, *31*, 1904735. [CrossRef]
89. Fu, H.; Zhang, J.; Li, Y.H.; Gong, L.; He, H.P.; Fang, Z.S.; Zhou, C.H.; Chen, J.L.; Fan, J.C. A facile interface engineering method to improve the performance of $FTO/ZnO/CsPbI_{3-x}Br_x$ ($x < 1$)/C solar cells. *J. Mater. Sci. Mater. Electron.* **2022**, *33*, 3711–3725. [CrossRef]
90. Fu, S.Q.; Wang, J.H.; Liu, X.H.; Yuan, H.B.; Xu, Z.X.; Long, Y.J.; Zhang, J.; Huang, L.K.; Hu, Z.Y.; Zhu, Y.J. Multifunctional liquid additive strategy for highly efficient and stable $CsPbI_2Br$ all-inorganic perovskite solar cells. *Chem. Eng. J.* **2021**, *422*, 130572. [CrossRef]
91. Yoon, S.M.; Min, H.; Kim, J.B.; Kim, G.; Lee, K.S.; Seok, S.I. Surface Engineering of Ambient-Air-Processed Cesium Lead Triiodide Layers for Efficient Solar Cells. *Joule* **2021**, *5*, 183–196. [CrossRef]
92. Li, Y.; Duan, L.; Zhang, Z.; Wang, H.; Chen, T.; Luo, J. Healing the defects in $CsPbI_3$ solar cells by $CsPbBr_3$ quantum dots. *Nano Res.* **2021**. [CrossRef]
93. Zhang, W.H.; Liu, H.; Qi, X.N.; Yu, Y.Y.; Zhou, Y.C.; Xia, Y.; Cui, J.S.; Shi, Y.Q.; Chen, R.; Wang, H.L. Oxalate Pushes Efficiency of $CsPb_{0.7}Sn_{0.3}IBr_2$ Based All-Inorganic Perovskite Solar Cells to over 14%. *Adv. Sci.* **2022**, *9*, 2106054. [CrossRef] [PubMed]
94. Wang, Q.; Xu, Y.; Zhang, L.; Yang, A.; Bai, T.; Liu, F.; Lyu, M.; Zhu, J. Guanidinium Thiocyanate Additive Engineering for High-Performance $CsPbIBr_2$ Solar Cells with an Efficiency of 10.90%. *ACS Appl. Energy Mater.* **2022**, *5*, 3110–3118. [CrossRef]
95. Liu, X.; Li, J.; Wang, X.; Yang, D. Inorganic lead-based halide perovskites: From fundamental properties to photovoltaic applications. *Mater. Today* **2022**, *61*, 191–217. [CrossRef]
96. Liu, C.; Li, W.; Zhang, C.; Ma, Y.; Fan, J.; Mai, Y. All-Inorganic $CsPbI_2Br$ Perovskite Solar Cells with High Efficiency Exceeding 13%. *J. Am. Chem. Soc.* **2018**, *140*, 3825–3828. [CrossRef] [PubMed]
97. Mariotti, S.; Hutter, O.S.; Phillips, L.J.; Yates, P.J.; Kundu, B.; Durose, K. Stability and Performance of $CsPbI_2Br$ Thin Films and Solar Cell Devices. *ACS Appl. Mater. Interfaces* **2018**, *10*, 3750–3760. [CrossRef]
98. Zhang, S.S.; Wu, S.H.; Chen, W.T.; Zhu, H.M.; Xiong, Z.Z.; Yang, Z.C.; Chen, C.L.; Chen, R.; Han, L.Y.; Chen, W. Solvent engineering for efficient inverted perovskite solar cells based on inorganic $CsPbI_2Br$ light absorber. *Mater. Today Energy* **2018**, *8*, 125–133. [CrossRef]
99. Yin, G.; Zhao, H.; Jiang, H.; Yuan, S.; Niu, T.; Zhao, K.; Liu, Z.; Liu, S. Precursor Engineering for All-Inorganic $CsPbI_2Br$ Perovskite Solar Cells with 14.78% Efficiency. *Adv. Funct. Mater.* **2018**, *28*, 1803269. [CrossRef]
100. Luo, P.; Xia, W.; Zhou, S.; Sun, L.; Cheng, J.; Xu, C.; Lu, Y. Solvent Engineering for Ambient-Air-Processed, Phase-Stable $CsPbI_3$ in Perovskite Solar Cells. *J. Phys. Chem. Lett.* **2016**, *7*, 3603–3608. [CrossRef]
101. Meng, Q.X.; Feng, J.Y.; Huang, H.T.; Han, X.P.; Zhu, Z.; Yu, T.; Li, Z.S.; Zou, Z.G. Simultaneous Optimization of Phase and Morphology of $CsPbBr_3$ Films via Controllable Ostwald Ripening by Ethylene Glycol Monomethylether/Isopropanol Bi-Solvent Engineering. *Adv. Eng. Mater.* **2020**, *22*, 2000162. [CrossRef]
102. He, Q.; Zhang, H.; Han, S.; Xing, Y.; Li, Y.; Zhang, X.; Wang, R. Improvement of green antisolvent-isopropanol and additive-thiourea on carbon based $CsPbIBr_2$ perovskite solar cells. *Mater. Sci. Semicond. Process.* **2022**, *150*, 106940. [CrossRef]
103. Wang, S.; Cao, F.; Sun, W.; Wang, C.; Yan, Z.; Wang, N.; Lan, Z.; Wu, J. A green Bi-Solvent system for processing high-quality $CsPbBr_3$ films in efficient all-inorganic perovskite solar cells. *Mater. Today Phys.* **2022**, *22*, 100614. [CrossRef]
104. Dong, C.; Han, X.X.; Li, W.H.; Qiu, Q.Q.; Wang, J.Q. Anti-solvent assisted multi-step deposition for efficient and stable carbon-based $CsPbI_2Br$ all-inorganic perovskite solar cell. *Nano Energy* **2019**, *59*, 553–559. [CrossRef]

105. Han, B.Q.; Zhang, L.; Cao, Y.W.; Li, B.Y.; Liu, Z.Y.; Xu, L.B.; Wang, P.; Lin, P.; Wu, X.P.; Cui, C. Antisolvent engineering on low-temperature processed $CsPbI_3$ inorganic perovskites for improved performances of solar cells. *Nanotechnology* **2021**, *32*, 185402. [CrossRef] [PubMed]
106. Saparbaev, A.; Zhang, M.L.; Kuvondikov, V.; Nurumbetova, L.; Raji, I.O.; Tajibaev, I.; Zakhidov, E.; Bao, X.C.; Yang, R.Q. High-performance $CsPbI_3$ perovskite solar cells without additives in air condition. *Sol. Energy* **2021**, *228*, 405–412. [CrossRef]
107. Teng, P.P.; Han, X.P.; Li, J.W.; Xu, Y.; Kang, L.; Wang, Y.R.Q.; Yang, Y.; Yu, T. Elegant Face-Down Liquid-Space-Restricted Deposition of $CsPbBr_3$ Films for Efficient Carbon-Based All-Inorganic Planar Perovskite Solar Cells. *ACS Appl. Mater. Interfaces* **2018**, *10*, 9541–9546. [CrossRef]
108. Zai, H.C.; Zhang, D.L.; Li, L.; Zhu, C.; Ma, S.; Zhao, Y.Z.; Zhao, Z.G.; Chen, C.F.; Zhou, H.P.; Li, Y.J.; et al. Low-temperature-processed inorganic perovskite solar cells via solvent engineering with enhanced mass transport. *J. Mater. Chem. A* **2018**, *6*, 23602–23609. [CrossRef]
109. Liu, X.; Tan, X.; Liu, Z.; Ye, H.; Sun, B.; Shi, T.; Tang, Z.; Liao, G. Boosting the efficiency of carbon-based planar $CsPbBr_3$ perovskite solar cells by a modified multistep spin-coating technique and interface engineering. *Nano Energy* **2019**, *56*, 184–195. [CrossRef]
110. Gao, B.W.; Meng, J. High efficiently $CsPbBr_3$ perovskite solar cells fabricated by multi-step spin coating method. *Sol. Energy* **2020**, *211*, 1223–1229. [CrossRef]
111. Wang, H.S.; Sun, J.; Gu, Y.S.; Xu, C.Q.; Lu, Y.W.; Hu, J.T.; Chen, T.; Zhu, C.F.; Luo, P.F. Solvent-engineering-processed $CsPbIBr_2$ inorganic perovskite solar cells with efficiency of similar to 11%. *Sol. Energy Mater. Sol. Cells* **2022**, *238*, 111640. [CrossRef]
112. Wang, H.L.; Liu, H.C.; Dong, Z.J.; Wei, X.Y.; Song, Y.F.; Li, W.P.; Zhu, L.Q.; Bai, Y.; Chen, H.N. Extracting ammonium halides by solvent from the hybrid perovskites with various dimensions to promote the crystallization of $CsPbI_3$ perovskite. *Nano Energy* **2022**, *94*, 106925. [CrossRef]
113. Zhong, T.T.; Zhang, C.; Hamukwaya, S.L.; Xu, W.S.; Tang, K.P.; Xu, X.; Sun, W.T.; Hao, H.Y.; Dong, J.J.; Liu, H.; et al. Efficient and stable carbon-based $CsPbBr_3$ solar cells added with PEABr additive. *Acta Phys. Sin.* **2022**, *71*, 028101. [CrossRef]
114. Chen, J.; Park, N.-G. Causes and Solutions of Recombination in Perovskite Solar Cells. *Adv. Mater.* **2019**, *31*, e1803019. [CrossRef]
115. Wang, J.-K.; Hou, H.-Y.; Li, Y.-Q.; Tang, J.-X. Recent advances in interface engineering of all-inorganic perovskite solar cells. *Nanoscale* **2020**, *12*, 17149–17164. [CrossRef]
116. Yan, L.; Xue, Q.F.; Liu, M.Y.; Zhu, Z.L.; Tian, J.J.; Li, Z.C.; Chen, Z.; Chen, Z.M.; Yan, H.; Yip, H.L.; et al. Interface Engineering for All-Inorganic $CsPbI_2Br$ Perovskite Solar Cells with Efficiency over 14%. *Adv. Mater.* **2018**, *30*, 1802509. [CrossRef]
117. Yue, M.; Su, J.; Zhao, P.; Lin, Z.H.; Zhang, J.C.; Chang, J.J.; Hao, Y. Optimizing the Performance of $CsPbI_3$-Based Perovskite Solar Cells via Doping a ZnO Electron Transport Layer Coupled with Interface Engineering. *Nano Micro Lett.* **2019**, *11*, 91. [CrossRef]
118. Yang, B.; Wang, M.; Hu, X.; Zhou, T.; Zang, Z. Highly efficient semitransparent $CsPbIBr_2$ perovskite solar cells via low-temperature processed In_2S_3 as electron-transport-layer. *Nano Energy* **2019**, *57*, 718–727. [CrossRef]
119. Zhu, W.; Chai, W.; Zhang, Z.; Chen, D.; Chang, J.; Liu, S.; Zhang, J.; Zhang, C.; Hao, Y. Interfacial TiO_2 atomic layer deposition triggers simultaneous crystallization control and band alignment for efficient $CsPbIBr_2$ perovskite solar cell. *Org. Electron.* **2019**, *74*, 103–109. [CrossRef]
120. Li, J.; Yang, J.; Ma, J.; Liang, J.; Liu, Y.; Hu, X.; Chen, C.; Yang, W.; Min, J.; Bao, Q.; et al. Minimizing Open-Circuit voltage deficit via interface engineering for highly efficient $CsPbI_2Br$ perovskite solar cells. *Chem. Eng. J.* **2021**, *417*, 129247. [CrossRef]
121. Pan, B.K.; Gu, J.H.; Xu, X.L.; Xiao, L.B.; Zhao, J.; Zou, G.F. Interface engineering of high performance all-inorganic perovskite solar cells via low-temperature processed TiO_2 nanopillar arrays. *Nano Res.* **2021**, *14*, 3431–3438. [CrossRef]
122. Guo, Z.; Teo, S.; Xu, Z.; Zhang, C.; Kamata, Y.; Hayase, S.; Ma, T. Achievable high Voc of carbon based all-inorganic $CsPbIBr_2$ perovskite solar cells through interface engineering. *J. Mater. Chem. A* **2019**, *7*, 1227–1232. [CrossRef]
123. Lu, G.; Wang, X.H.; Du, J.; Zhang, M.; Gao, Y.L.; Liu, Y.B.; Ma, J.; Lin, Z.H. Enhancing Perovskite Solar Cell Performance through Surface Engineering of Metal Oxide Electron-Transporting Layer. *Coatings* **2020**, *10*, 46. [CrossRef]
124. Wang, J.; Wu, X.; Liu, Y.Z.; Xue, Q.F.; Yip, H.L.; Jen, A.K.Y.; Zhu, Z.L. Interface Engineering for All-Inorganic $CsPbIBr_2$ Perovskite Solar Cells with Enhanced Power Conversion Efficiency over 11%. *Energy Technol.* **2021**, *9*, 2100562. [CrossRef]
125. Wang, K.; Zhang, Z.; Wang, L.; Chen, K.; Tao, L.; Zhang, Y.; Zhou, X. Commercial Carbon-Based all-Inorganic Perovskite Solar Cells with a High Efficiency of 13.81%: Interface Engineering and Photovoltaic Performance. *ACS Appl. Energy Mater.* **2021**, *4*, 3255–3264. [CrossRef]
126. Chai, W.; Zhu, W.; Zhang, Z.; Liu, D.; Ni, Y.; Song, Z.; Dong, P.; Chen, D.; Zhang, J.; Zhang, C.; et al. $CsPbBr_3$ seeds improve crystallization and energy level alignment for highly efficient $CsPbI_3$ perovskite solar cells. *Chem. Eng. J.* **2023**, *452*, 139292. [CrossRef]
127. Liu, C.; Li, W.Z.; Chen, J.H.; Fan, J.D.; Mai, Y.H.; Schropp, R.E.I. Ultra-thin MoOx as cathode buffer layer for the improvement of all-inorganic $CsPbIBr_2$ perovskite solar cells. *Nano Energy* **2017**, *41*, 75–83. [CrossRef]
128. Zhou, L.; Guo, X.; Lin, Z.H.; Ma, J.; Su, J.; Hu, Z.S.; Zhang, C.F.; Liu, S.Z.; Chang, J.J.; Hao, Y. Interface engineering of low temperature processed all-inorganic $CsPbI_2Br$ perovskite solar cells toward PCE exceeding 14%. *Nano Energy* **2019**, *60*, 583–590. [CrossRef]
129. Zong, Z.H.; He, B.L.; Zhu, J.W.; Ding, Y.; Zhang, W.Y.; Duan, J.L.; Zhao, Y.Y.; Chen, H.Y.; Tang, Q.W. Boosted hole extraction in all-inorganic $CsPbBr_3$ perovskite solar cells by interface engineering using MoO2/N-doped carbon nanospheres composite. *Sol. Energy Mater. Sol. Cells* **2020**, *209*, 110460. [CrossRef]

130. Xue, Q.F.; Liu, M.Y.; Li, Z.C.; Yan, L.; Hu, Z.C.; Zhou, J.W.; Li, W.Q.; Jiang, X.F.; Xu, B.M.; Huang, F.; et al. Efficient and Stable Perovskite Solar Cells via Dual Functionalization of Dopamine Semiquinone Radical with Improved Trap Passivation Capabilities. *Adv. Funct. Mater.* **2018**, *28*, 1707444. [CrossRef]
131. Ding, Y.; He, B.L.; Zhu, J.W.; Zhang, W.Y.; Su, G.D.; Duan, J.L.; Zhao, Y.Y.; Chen, H.Y.; Tang, Q.W. Advanced Modification of Perovskite Surfaces for Defect Passivation and Efficient Charge Extraction in Air-Stable $CsPbBr_3$ Perovskite Solar Cells. *ACS Sustain. Chem. Eng.* **2019**, *7*, 19286–19294. [CrossRef]
132. Yang, S.Z.; Wang, L.; Gao, L.G.; Cao, J.M.; Han, Q.J.; Yu, F.Y.; Kamata, Y.; Zhang, C.; Fan, M.Q.; Wei, G.Y.; et al. Excellent Moisture Stability and Efficiency of Inverted All-Inorganic $CsPbIBr_2$ Perovskite Solar Cells through Molecule Interface Engineering. *ACS Appl. Mater. Interfaces* **2020**, *12*, 13931–13940. [CrossRef] [PubMed]
133. Zhu, J.W.; Liu, Y.; He, B.L.; Zhang, W.Y.; Cui, L.F.; Wang, S.D.; Chen, H.Y.; Duan, Y.Y.; Tang, Q.W. Efficient interface engineering of N, N′-Dicyclohexylcarbodiimide for stable HTMs-free $CsPbBr_3$ perovskite solar cells with 10.16%-efficiency. *Chem. Eng. J.* **2022**, *428*, 131950. [CrossRef]
134. Du, Y.T.; Wu, J.H.; Li, G.D.; Wang, X.B.; Song, Z.Y.; Deng, C.Y.; Chen, Q.; Zou, Y.; Sun, W.H.; Lan, Z. Bulky ammonium iodide and in-situ formed 2D Ruddlesden-Popper layer enhances the stability and efficiency of perovskite solar cells. *J. Colloid Interface Sci.* **2022**, *614*, 247–255. [CrossRef] [PubMed]
135. Xu, Y.; Li, G.; Li, R.; Jing, Y.; Zhang, H.; Wang, X.; Du, Z.; Wu, J.; Lan, Z. PbS/CdS heterojunction thin layer affords high-performance carbon-based all-inorganic solar cells. *Nano Energy* **2022**, *95*, 106973. [CrossRef]
136. Zou, Y.; Cao, F.; Chen, P.; He, R.; Tong, A.; Yin, C.; Lan, Z.; Sun, W.; Wu, J. Stable and highly efficient all-inorganic $CsPbBr_3$ perovskite solar cells by interface engineering with NiO NCs modification. *Electrochim. Acta* **2022**, *435*, 1065–1074. [CrossRef]
137. Liao, G.Q.; Duan, J.L.; Zhao, Y.Y.; Tang, Q.W. Toward fast charge extraction in all-inorganic $CsPbBr_3$ perovskite solar cells by setting intermediate energy levels. *Sol. Energy* **2018**, *171*, 279–285. [CrossRef]
138. Xu, H.Z.; Duan, J.L.; Zhao, Y.Y.; Jiao, Z.B.; He, B.L.; Tang, Q.W. 9.13%-Efficiency and stable inorganic $CsPbBr_3$ solar cells. Lead-free $CsSnBr_{3-x}I_x$ quantum dots promote charge extraction. *J. Power Sources* **2018**, *399*, 76–82. [CrossRef]
139. Li, Q.H.; Bai, J.K.; Zhang, T.T.; Nie, C.; Duan, J.L.; Tang, Q.W. CdZnSe@ZnSe colloidal alloy quantum dots for high-efficiency all-inorganic perovskite solar cells. *Chem. Commun.* **2018**, *54*, 9575–9578. [CrossRef]
140. Bian, H.; Bai, D.; Jin, Z.; Wang, K.; Liang, L.; Wang, H.; Zhang, J.; Wang, Q.; Liu, S. Graded Bandgap $CsPbI_{2+x}Br_{1-x}$ Perovskite Solar Cells with a Stabilized Efficiency of 14.4%. *Joule* **2018**, *2*, 1500–1510. [CrossRef]
141. Chen, Z.; Yang, M.; Li, R.; Zang, Z.; Wang, H. Double-Side Interface Engineering Synergistically Boosts the Efficiency of Inorganic $CsPbIBr_2$ Perovskite Solar Cells Over 12%. *Adv. Opt. Mater.* **2022**, *10*, 2200802. [CrossRef]
142. Shi, L.; Yuan, H.; Zhang, Y.; Sun, X.; Duan, L.; Li, Q.; Huang, Z.; Ban, X.; Zhang, D. Novel C_3N_4-Assisted Bilateral Interface Engineering for Efficient and Stable Perovskite Solar Cells. *Langmuir* **2022**, *38*, 12390–12398. [CrossRef] [PubMed]
143. Wang, J.; Zhang, J.; Zhou, Y.; Liu, H.; Xue, Q.; Li, X.; Chueh, C.-C.; Yip, H.-L.; Zhu, Z.; Jen, A.K.Y. Highly efficient all-inorganic perovskite solar cells with suppressed non-radiative recombination by a Lewis base. *Nat. Commun.* **2020**, *11*, 1329. [CrossRef] [PubMed]